IMPACT OF PRESSURE EQUALIZATION SLOT IN FLOW CHANNEL INSERT ON TRITIUM TRANSPORT IN A DCLL-TYPE POLOIDAL DUCT

H. Zhang, A. Ying, M. Abdou

Mechanical and Aerospace Engineering Dept., UCLA, Los Angeles, CA 90095, USA, zhjbook@gmail.com

A SiC-based flow channel insert (FCI) is used as an electrical and thermal insulator in the Dual Coolant Lead Lithium (DCLL) blanket. To reduce the stress of the FCI structural material, the pressure equalization slot (PES) is implemented in the FCI wall. However, the PES affects the tritium transfer behavior and loss rate. Therefore it is important to examine the tritium loss rate and ensure it remains below an allowable limit. In the present study, we analyze tritium transport and quantify the tritium loss rate in a front duct of the DCLL-type outboard blanket where PbLi moves poloidally. Three types of poloidal ducts have been considered: one without the PES, one with the PES in the wall parallel to the magnetic field and one with the PES in the wall perpendicular to the magnetic field. Tritium concentration fields are obtained by solving a fully 3-D problem with appropriate boundary conditions at various interfaces. Results show a high tritium concentration at the location of reversed flow when a PES was located in the wall parallel to the field. Furthermore, when any PES was introduced, the PES changed the velocity profiles and thus changed the tritium concentrations in the core and gaps, which increases the tritium losses from 1.244% to 1.413% under the calculation conditions.

I. INTRODUCTION

Proper control of tritium transport and permeation in fusion blankets are important features contributing to the achievement of tritium self-sufficiency as well as being necessary to accurately characterize tritium inventory and losses. In the liquid metal (LM) blanket, multiple tritium transport processes have to be considered simultaneously because of the multi-material domains. The processes include: tritium diffusion and convection in the flowing LM, transfer across the liquid/solid interface, and diffusion through the structure. Tritium transport is also combined with magnetohydrodynamic (MHD) effects, which cause flow redistribution. Any flow redistribution affects the tritium concentration profile and thus the permeation rate. To reduce the stress in the FCI structure material, a PES is utilized at the FCI wall to balance the pressure inside (core) and outside (gaps) of the FCI. However, the PES affects the tritium transfer behavior and loss rate. First, it provides a path for tritium to migrate between the core and the gap. The second is that the PES changes the local MHD velocity distribution that in turn affects tritium diffusion and convection. The purpose of this paper is to develop mathematical and computational models for tritium transport in multi-region liquid PbLi DCLL blanket configurations and evaluate the effect of PES on tritium permeation and distributions.

Currently, TMAP7 (Ref. 1) is the reference tool for the simulation of the permeation phenomenon in ITER. Unfortunately it has an important disadvantage: TMAP7 is only a 1D program. That makes it not completely adequate for the 3D blanket geometries and also makes it difficult to estimate tritium transport in flowing liquid metal that is an inherently three-dimensional flow. In this study, we formulate the problem in 3D and numerically solve the complete set of governing equations with appropriate boundary conditions at various interfaces. The tritium transport is simulated for a front duct in a DCLL-type outboard blanket where PbLi moves poloidally. Tritium concentration and permeation flux are presented and the PES effects are evaluated.

II. FORMULATION OF THE PROBLEM

The tritium transport model presented in Fig. 1 includes the multiple tritium transport processes:

- Tritium generation in LM core and gaps
- Tritium convection and diffusion in flowing LM
- Tritium movement through the LM/FCI interface
- Diffusion tritium in FCI
- Tritium migration through PES
- Tritium movement through the LM/ferritic steel (FS) structure interface
- Diffusion of tritium through the FS structure.
- Tritium desorption and recombination at FS/He coolant interface
- Tritium transfer & trapping into He bubbles

In any given situation, the process that contributes the most to the tritium transport within the LM blanket depends on the specific material properties (e.g. tritium

solubility and diffusivity), operating temperature range and the flow distribution under consideration.

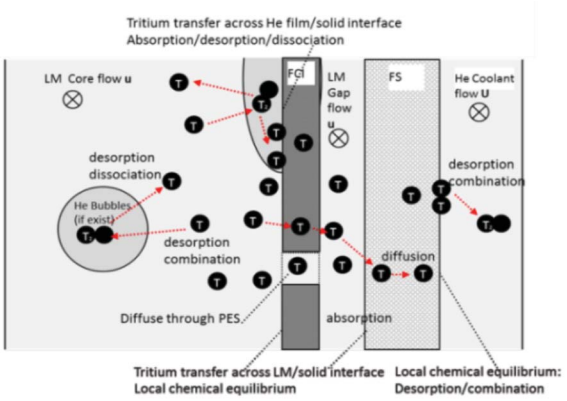

Fig. 1. The schematic of the tritium transport model shows all the sources and transportation modes of tritium in a liquid metal breeder blanket unit.

For tritium transport modeling in the liquid PbLi, we assume tritium does not alter liquid metal properties nor flow behavior. Hence, general passive scalar transport equation for the concentration of species s, $c_s\,(mol/m^3)$, can be expressed as: [1]

$$\partial c_s(\mathbf{x},t)/\partial t = -\nabla\cdot\mathbf{J}_s(\mathbf{x},t) + S_s(\mathbf{x},t) + \\ -\sum_k(\partial c_s^{t_k}/\partial t + \nu_s c_s^{t_k}) - \nu_s c_s + \sum_m \nu_m^s(c_m + \sum_k c_m^{t_k}) \quad (1)$$

Where S_s is the local source rate per unit volume (mol/ms^3), The superscript t represents trapped atoms, k denotes different kinds of trap sites, ν_s is the radioactive decay frequency of species "s" atoms, ν_m^s is the radioactive decay frequency of species, m, atoms that decay to species, s, and $\mathbf{J}_s$ is the flux of dissolved atoms "s", which is given by

$$\mathbf{J}_s = -D(T)\nabla c_s - (D(T)Q_s^* c_s/kT^2)\nabla T + c_s\mathbf{u} \quad (2)$$

Where D is the diffusivity, $\mathbf{u}$ is the advection speed, Q^* is Soret coefficient, and T is the local temperature. The first term represents the flux of species s due to concentration gradient; the second term represents the flux of species s due to temperature gradient and the third term results from the effects of bulk flow.

In the present study, the radioactive decay, the trap, and the flux associated with temperature gradients are assumed to be much smaller compared to those due to concentration gradients and are therefore omitted. We also ignored the helium bubble effect because this phenomenon is not confirmed in DCLL blanket concepts and a lack of experimental data.

Let's define c_{T_LM}, c_{T_FS}, c_{T_FCI} and c_{T2_HC} as the tritium concentration in the LM, FS structure, FCI and He coolant, respectively. In doing so, the following mass balance equations can be formulated in these domains:

$$\partial c_{T\_LM}/\partial t = \nabla\cdot(D_{LM}\nabla c_{T\_LM}) - \mathbf{u}_{LM}\nabla c_{T\_LM} + S_T \quad (3)$$

$$\partial c_{T\_FCI}/\partial t = \nabla\cdot(D_{FCI}\nabla c_{T\_FCI}) \quad (4)$$

$$\partial c_{T\_FS}/\partial t = \nabla\cdot(D_{FS}\nabla c_{T\_FS}) \quad (5)$$

$$\partial c_{T2\_HC}/\partial t = \nabla\cdot(D_{HC}\nabla c_{T2\_HC}) - \mathbf{U}_{HC}\nabla c_{T2\_HC} \quad (6)$$

Where D_{LM}, D_{FS}, D_{FCI}, and D_{HC} are the diffusivities (m^2/s) in the respective regions, $\mathbf{u}_{LM}$ and $\mathbf{U}_{HC}$ are the velocities (m/s) in the LM and He coolant, t is time (s) and S_T is the tritium generation rate $(mol/m^3 s)$.

To obtain the convective part of the flux in the PbLi region, the equations for the steady state, laminar, incompressible, viscous, MHD flow are given by: [2]

$$\nabla\cdot\mathbf{u} = 0 \quad (7)$$

$$\frac{\partial\rho\mathbf{u}}{\partial t} + \mathbf{u}\nabla\rho\mathbf{u} = \mu\nabla^2\mathbf{u} - \nabla p + \mathbf{j}\times\mathbf{B} \quad (8)$$

$$\nabla\cdot\mathbf{j} = 0 \quad (9)$$

$$\mathbf{j} = \sigma(-\nabla\phi + \mathbf{u}\times\mathbf{B}) \quad (10)$$

By combining equations (9) and (10), a Poisson equation for the electric potential is obtained:

$$\nabla\cdot(\sigma\nabla\phi) = \nabla\cdot(\sigma\mathbf{u}\times\mathbf{B}) \quad (11)$$

Where the variables B, j, ϕ, ρ, σ and μ denote the magnetic field, current density, electric potential, density, electric conductivity and the viscosity, respectively.

To supplement the transport equations, a set of boundary conditions expressing species flux and chemical potential balance are applied at material interfaces.

At the LM/FS and LM/FCI interface, we apply Sievert's law and impose continuity of partial pressure. This leads to the concentration discontinuities at interfaces.

$$\frac{c_{T\_FS}}{c_{T\_LM}} = \frac{K_{s\_FS}}{K_{s\_LM}}\frac{c_{T\_FCI}}{c_{T\_LM}} = \frac{K_{s\_FCI}}{K_{s\_LM}} \quad (12)$$

Where K_{S_LM}, K_{S_FS} and K_{S_FCI} are the solubility of tritium in LM, FS, and FCI.

To ensure continuity of fluxes, we also apply

$$(-D_{LM}\nabla c_{T\_LM} + c_{T\_LM}\mathbf{u}_{LM})\cdot\mathbf{n} = (-D_{FS}\nabla c_{T\_FS})\cdot\mathbf{n} \quad (13)$$

$$(-D_{LM}\nabla c_{T\_LM} + c_{T\_LM}\mathbf{u}_{LM})\cdot\mathbf{n} = (-D_{FCI}\nabla c_{T\_FCI})\cdot\mathbf{n} \quad (14)$$

At FS/HC interface, the species flux is determined by the surface recombination rate:

$$(-D_{FS}\nabla c_{T\_FS})\cdot\mathbf{n} = K_r c_{T\_FS}^2 \quad (15)$$

Where K_r is the recombination coefficient (m^4/s).

III. NUMERICAL RESULTS AND DISCUSSION

In this work, we analyzed tritium transport in a front duct of a DCLL-type outboard blanket where PbLi moves poloidally.[3] Three types of poloidal ducts have been considered: one without the PES, one with the PES in the wall parallel to the magnetic field and one with the PES in the wall perpendicular to the field. A sketch of the cross-sectional area of the liquid metal blanket channel with FCI is shown in Fig. 2.

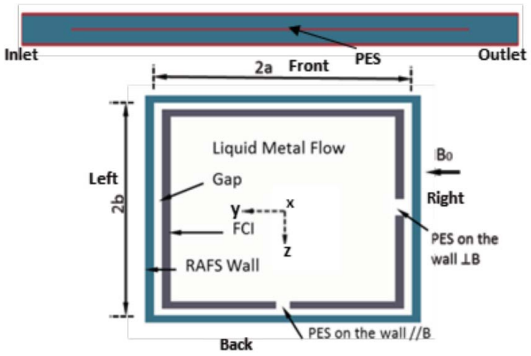

Fig. 2. The cross-section drawing of the blanket duct shows the PES openings. Here the PES is opened from x=0.1m to 0.9m and with 2a=0.06m, 2b=0.06m, RAFS wall 0.002m, FCI 0.002m, PES 0.003m, Gap 0.002m

The velocity field is obtained by performing a 3D simulation with magnetic field strength of1.852*T*. The electrical conductivity $\sigma_{LM}=7\times10^5\Omega^{-1}m^{-1}$, $\sigma_{FS}=1.46\times10^6\Omega^{-1}m^{-1}$, $\sigma_{FCI}=5\times10^2\Omega^{-1}m^{-1}$. 216×195×164 non-uniform meshes are used to discretize the geometry with 216 non-uniformly distributed in the x-direction. A uniform velocity of U0=0.0675*m/s* is given as inlet boundary condition, and the pressure at outlet is specified as zero. Non-slip boundary conditions are applied on the solid walls. Velocity distributions at the cross-section of x=0.5m are plotted in Fig. 3. In Fig. 3(a) for the case of no PES, when we set y=0, we see the velocity profile has a relatively high velocity in the gaps parallel to the magnetic field and a very low velocity in the gaps perpendicular to the field. When any PES is introduced, the high velocities in the front and back gaps disappeared. Figure 3 also shows that when a PES is opened parallel to the field, we see a strong reversed flow at the location of the PES due to a large component of Lorentz force along the negative main flow direction. In Fig. 3(b), we have set z=0. In the figure we see flat-shaped velocity profiles in the core and very low velocities in the left and right gaps. For the case of a PES opening perpendicular to the field, the velocity is not symmetric. It is higher in the right gap than left gap, and a velocity drop in the core near the location of PES is observed. These velocity profiles match earlier observations for various FCI flows reported in.[4] A full three dimensional plot of the results from the cross-section at x=0.5 is also given in Fig. 4 for clarity.

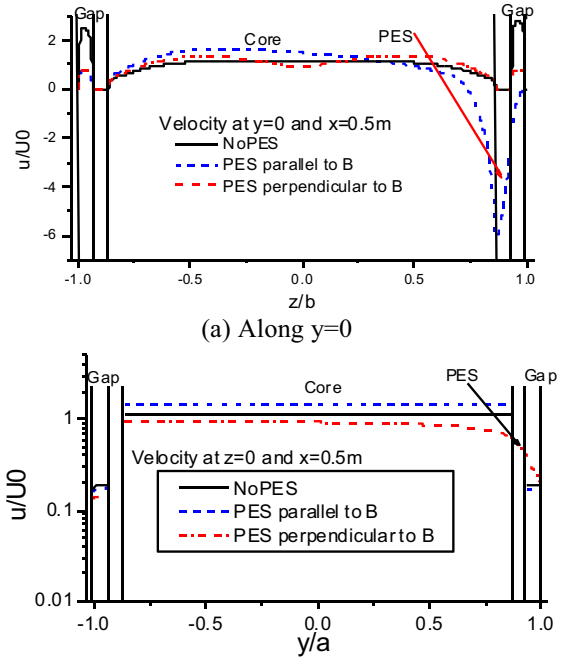

Fig. 3. Velocities at the cross-section of x=0.5m. (a) Along y=0, it shows a strong reversed flow near the insert for the case of PES is opened parallel to the field. (b) Along z=0, it shows flat-shaped velocity profiles in the core and very low velocities in the left and right gaps.

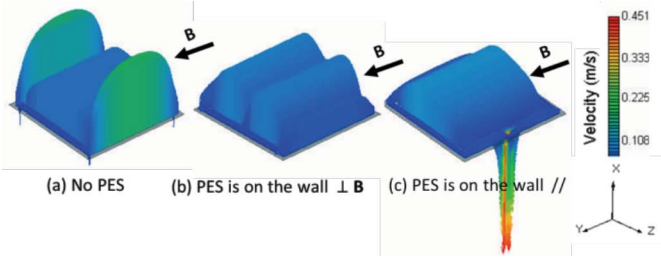

Fig. 4. Velocity profiles at across section of x=0.5m for various PES configurations.

The computer code to solve the FCI flow field has been validated by solving Ming-Jiu Ni's case.[4] In Ni's case, PES is opened parallel to the magnetic field and GaInSn was selected as the liquid metal with 2a = 34mm and 2b = 40mm. The velocity profile at the cross-section

of x=0.5m as seen in Fig. 5 shows good agreement with Ni's solution.

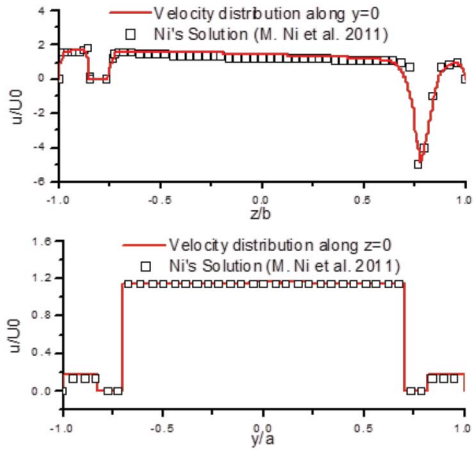

Fig. 5. Comparison of velocity at y-z cross-section.

Tritium concentration fields are obtained by our recently developed code, which has been validated with some experimental data.[5] It solves a fully 3-D problem with aforementioned boundary conditions at various interfaces. Additionally, zero concentration is given at inlet and convective flux boundary condition is given at outlet. Tritium generation rate[6] is plotted in Fig. 6.

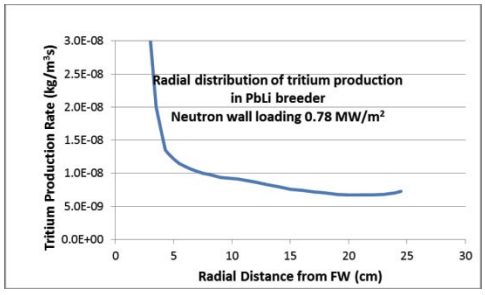

Fig. 6. Tritium generation rate shows a non-uniform profile along the radial distance from FW.

Tritium diffusion coefficients and Sievert's constants are dependent on temperature and activation energy. There is a dramatic discrepancy between the values computed by data presented in various references.[7] This study used the following values, $D_{LM}=1.3\times10^{-9}m^2/s$, $K_{s\_LM}=1.02\times10^{-3}mol/m^3Pa^{1/2}$.

Figure 7 shows the tritium concentration profiles at the cross-section of x=0.5m for the three different PES configurations. Without a PES opening in FCIs, the tritium concentrations in those gaps aligned perpendicular to the magnetic field are higher than the other two gaps and the core as seen in Fig. 7(a). Tritium concentration increasing in the positive z direction of the gaps reflects the decreased tritium generation rate away from the front wall. Also, because of the high velocity jet found in the front and back gap, tritium concentration near the front wall is reduced. With a PES in a wall perpendicular to the magnetic field, the concentrations in the right gap became lower than in the left gap, which reflected the non-symmetric velocity profile described in Fig. 3(b). Also, a weak concentration jump was formed around the PES as seen in Fig. 7(b). With a PES in a wall parallel to the magnetic field, such as in Fig. 7(c), we see a high tritium concentration in the bulk area near the location of the PES, which is due to the reversed flow at that location.

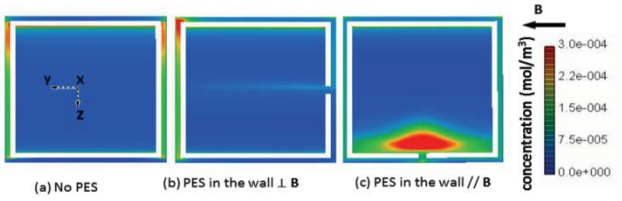

Fig. 7. Tritium concentrations at across section of x=0.5m for various PES configurations.

Figure 8 also demonstrates the features seen in Fig. 7(c). In Fig. 8, we are seeing the tritium distribution at the cross-section of y=0 along the flow direction. Tritium accumulated in the core area above the PES. It is also interesting to notice that tritium accumulated near the back wall behind the PES end as marked by the cycle region and resulted in local tritium permeation jump as showed in Fig. 11(c). This is due to very low velocities in that area as shown by the arrow plot of velocity in Fig. 8.

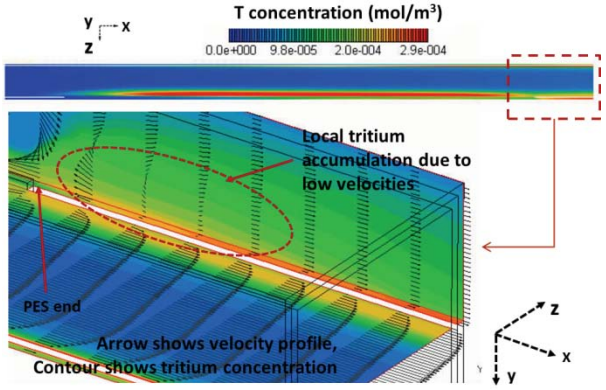

Fig. 8. Tritium concentration near the outlet (bottom) and at the cross-section of y=0 (top) with PES wall parallel to the field. Here Tritium accumulated in the core area above the PES and in the back gap behind the PES end.

When we plot the tritium concentration at the same cross-sections as Fig. 3, we see the interesting coupling between velocity and tritium concentration. This is done in Figs. 9 and 10 where the tritium concentrations are

plotted along y=0 and z=0, respectively, at the cross-section of x=0.5m. These tritium concentrations curves correspond to the velocity profiles seen above. The important conclusion is that high tritium concentrations are always associated with low-speed velocities. For example, in the front and back gaps, as seen in Fig. 9, the case of no PES (which had a relatively high velocity profile) gives the lowest tritium concentrations. The highest concentrations are observed when the PES is opened parallel to the field and occurs complementary to the velocity decrease shown in Fig. 3.

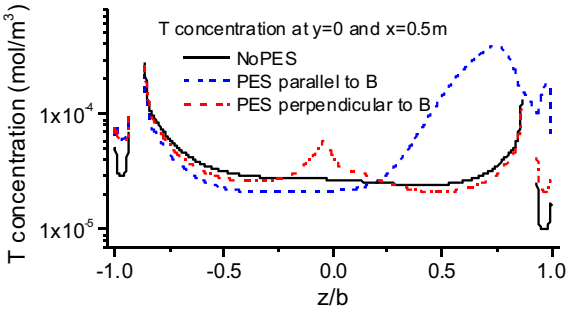

Fig. 9. Tritium concentrations along the line of **y=0m** at the cross-section of x=0.5m shows a high tritium concentration in the bulk area near the location of the PES for the case of PES is opened parallel to the field

Along z=0, as shown in Fig. 10, tritium concentrations in the left and right gaps are higher than in the core for all three cases. The case of no PES gives a higher tritium concentration and the case of the PES opening parallel to the field gives a lower concentration. When the PES is opened perpendicular to the field, it results in the highest tritium concentration in the left gap and a lowest concentration in the right gap compared to other two cases. Fig. 9 and 10 showed that the tritium transport across the PbLi is not only governed by diffusion but can be dominated by the advective movement of the bulk PbLi.

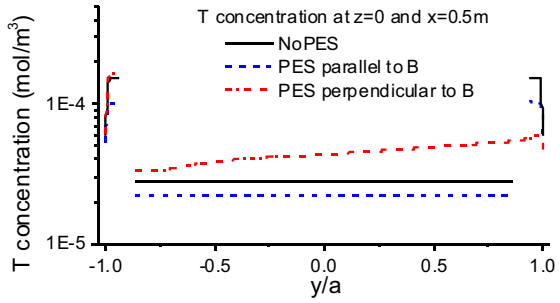

Fig. 10. Tritium concentrations along the line of **z=0m** at the cross-section of x=0.5m shows higher concentrations in the gaps than in the core.

Figure11 shows the tritium permeation per unit length through the front, back, left and right LM_FS wall. For the case of no PES in the FCI, Fig. 11(a), tritium permeation is higher through the left and right walls than the front and back walls due to high concentrations in the left and right gaps, as highlighted in Fig. 7(a). Tritium permeation through front wall is higher than the back wall because of the high tritium generation rate in the front gap. With a PES opening in the right wall, which is perpendicular to the magnetic field, Fig. 11(b), the front wall has the highest permeation flux and back wall has the lowest value. There is also a difference between the left wall and right wall. Tritium permeation is lower through the wall on the PES side because of lower tritium concentration in the right gap. With a PES opening in the back wall parallel to the magnetic field, tritium permeation is higher through the front wall as seen in Fig. 11(c), while the permeation through the back wall (where the PES is located) increases compared to the other two cases. It is also interesting to notice that there is a tritium permeation jump through back wall behind the end of PES. This is attributed to high tritium concentration in that area due to low velocities as described with Fig. 8.

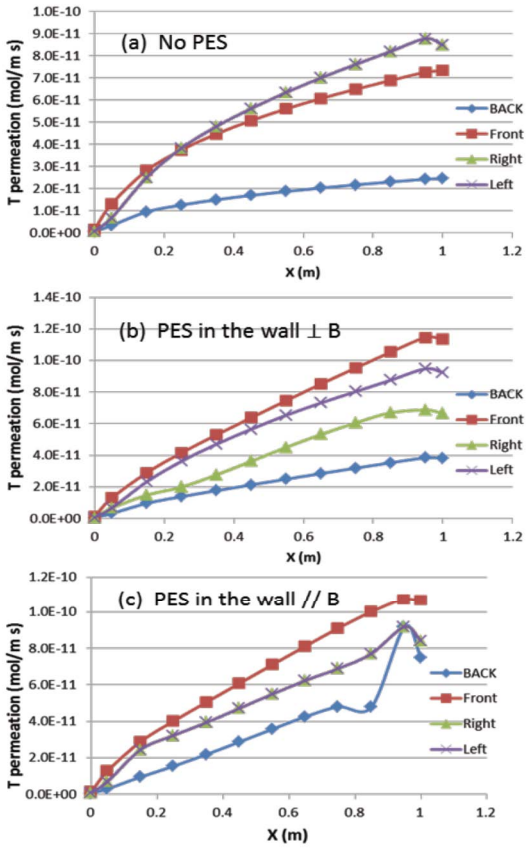

Fig. 11. Tritium permeation per unit length through the LM_FS walls (the front, back, left and right walls).

Figure12 shows the total tritium permeation through the four LM-FS walls. It can be seen that tritium permeation is higher when PES is opened in the wall parallel to the magnetic field. The overall permeation losses for the three different PES configurations are summarized in Table I. For the case without a PES under the given conditions, tritium loss is 1.244% of the tritium production, which confirms earlier results (tritium permeation loss is less than 2% of the total tritium production) for a DCLL duct flow without PES.[8] When the PES is opened perpendicular to the magnetic field, it results in a higher tritium loss of 1.321% of the tritium production. The case of PES opening parallel to the field gives a highest tritium loss of 1.413% of tritium production. The amount of increase in tritium permeation is minimized because the PES is located in the back wall where tritium generation rate is lower.

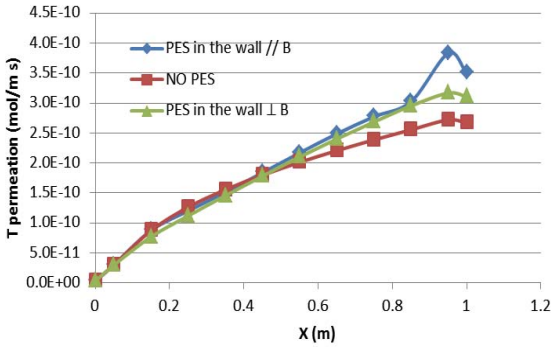

Fig. 12. Total tritium permeation per unit length through LM-FS walls

TABLE I. Tritium Losses for Three PES Configurations

	No PES	PES in the wall // B	PES in the wall B
T generation (mol/s)	1.412×10^{-8}	1.411×10^{-8}	1.413×10^{-8}
T permeation (mol/s)	1.756×10^{-10}	1.993×10^{-10}	1.866×10^{-10}
Loss percentage	1.244%	1.413%	1.321%

IV. CONCLUSIONS

In this paper, we developed the framework of the predictive capability for tritium transport in a multi-region liquid PbLi DCLL blanket configuration. The presence of PES on tritium permeation and distribution are investigated numerically. Results show that PES in the FCIs changed the velocity profiles and thus changed the tritium concentrations in the core and gaps. High tritium concentrations are always associated with low-speed velocities. With a PES in a wall parallel to the magnetic field, results show a high tritium concentration in the bulk near the location of the PES due to the reversed flow. Under the given conditions, the case of without PES gives a lowest tritium loss of 1.244% of the tritium production, while tritium loss increased nearly 14 percent for the case of PES opening parallel to the magnetic field. It results in a highest tritium loss of 1.413 % of the tritium production.

ACKNOWLEDGMENTS

This work was supported by the U. S. Department of Energy Contract DE-FG03-ER52123.

REFERENCES

1. G. R. LONGHURST, "TMAP7 User Manual," *Idaho National Engineering and Environmental Laboratory Bechtel BWXT Idaho*, LLC, (2004).
2. C. MISTRANGELO and L. BUHLER, "Electric Flow Coupling in the HCLL Blanket Concept," *Fusion Eng. Des*., **83**, 1232-1237 (2008).
3. P. NORAJITRA, L. BUHLER, et al., "Conceptual Design of the Dual-coolant Blanket in the Frame for the EU Power Plant Conceptual Study (TW2-TRP-PPCS12D)," *Forschungszentrum Karlsruhe Report FZKA*, 6780 (2002).
4. M. Ni, S. XU, Z. WANG and N. ZHANG, "Simulation of MHD Flows in Liquid Metal Blanket with Flow Channel Insert," *Fusion Sci. Technol.,* **60**, 292-297 (2011).
5. H. ZHANG, A. YING, M. A. ABDOU, "Integrated Simulation of Tritium Permeation in Solid Breeder Blankets," *Fusion Eng. Des*., **85**, 1711–1715(2010).
6. P. BATISTONIA, U. FISCHERB, K. OCHIAIC, L. PETRIZZIA, K. SEIDELD, M. YOUSSEFE, "Neutronics and Nuclear Data Issues in ITER and Their Validation," *Fusion Eng. Des*., **83**, 834-841 (2008).
7. E. MAS DE LES VALLS, L.A. SEDANO, L. BATET, I. RICAPITO, A. AIELLO, O. GASTALDI and F. GABRIEL, "Lead-lithium Eutectic Material Database for Nuclear Fusion Technology," *J. Nucl. Mater.,* **376**, 353-357 (2008).
8. M.J. PATTISON, S. SMOLENTSEV, R. MUNIPALLI, M. A. ABDOU, "Tritium Transport in Poloidal Flows of a DCLL Blanket," *Fusion Sci. Technol.*, **60**, 809 (2011).